Available online at www.elixirpublishers.com (Elixir International Journal)

Electrical Engineering

Elixir Elec. Engg. 117 (2018) 50512-50521

ISSN: 2229-712X

Enhancing the Load Ability of Congested Power Systems' Transmission Lines Using FACTS Technology

Okwuelu Nnameka[1], Onyedikachi Samuel.N[2] and Udeze Chidiebele .C.[3]

[1]Research and Development, Department of Electronics Development Institute, Awka, Anambra State, Nigeria.

[2]Department of Electrical Engineering, Nnamdi Azikiwe University, Awka, Anambra State, Nigeria.

[3]Electronic Engineering Department, University of Nigeria Nsukka.

ARTICLE INFO

Article history:

Received: 28 February 2018;

Received in revised form:

10 April 2018;

Accepted: 21 April 2018;

Keywords

FACTS Devices,

Reactive Power,

Power Systems,

Static Var Compensators,

Power Transfer Capacity.

ABSTRACT

Congestion in the power system transmission network has been a major constraint towards making active power available to the consumers. One of the conventional and long term methods but capital intensive to alleviating this problem is by adding new, expanding or reinforcing existing transmission facility. In this work, an interim, short term and cost effective measure – the use of TCSC and SVC in enhancing loadability of congested power transmission line was presented. The Nigerian Interconnected Power System – 330 kV bus power transmission network was used as a baseline and NEPLAN[1] – a power system software was used to run load flow analysis on the network in four stages: a baseline load flow analysis on the network to identify areas of constraints, a load flow analysis with TCSC located in-between optimal nodes, load flow analysis with SVC located at optimal nodes and then, a load flow analysis in the presence of TCSC and SVC on the network. The impact of these activities were investigated and the results showed that under baseline condition, low voltage violations occurred at [1]Gombe, Jos, Kaduna, Kano, Kebbi, Maiduguri, Makurdi, and Sokoto bus stations with percentage bus voltage of 65.77%, 72.83%, 79.96%, 62.29%, 89.63%, 65.37%, 79.46%, and 89.07% respectively; well below the reference percentage bus voltage profile of 90%. The combined services of TCSC and SVC as proposed, remedied the violations with a corresponding percentage bus voltages of 94.83%, 99.50%, 96.84%, 99.50%, 99.09%, 94.55%, 95.48%, and 99.50% respectively. With the presence of TCSC & SVC, total active power loss on the network was reduced from 108.76MW to 59.18MW (46%), and total reactive power loss, from 931.19MVar to 505.92Mvar (46%). Loadability was greatly enhanced on the lines with TCSC and the neighboring lines. For instance, in Makurdi-Jos line, there was active power increase from 212.60MW to 300.61MW, creating about 41% capacity margin; and Kaduna-Jos line, from 45.50MW to 132.97MW, about 195% capacity margin. The overall impact is in the network is that overloaded and congested lines were greatly relieved.

1. Introduction

The supply of electricity at competitive unit price, in sufficient quantity and quality, with safe and reliable supply through reliable equipment, system structures and devices is indispensable for competitive electricity markets and economic development of industries, regions and countries [11]. This is the prevailing consensus among power sector stakeholders. While recent trend advocate distributed or embedded generation through renewable energy penetration, the role of the transmission facility as determined by its operational state in evacuating power from generation to load centers in the current electric network structure and practice cannot be overemphasized. The availability of electric power from a power system with adequate or redundant generation capacity to consumers at the load centers is limited by the state and capacity of the transmission facilities. For instance, power systems operated at or near their thermal limits are vulnerable to faults or eventual system collapse. This could be due to insulation degradation of transmission facilities and the inevitable damage or preventive relay operations to keep them safe and offline.

This offline status of system components dwindles systems' degree of reliability, yet an interconnected network with adequate alternate power evacuating routes would subject the remaining online components to operations beyond their safe operational limits: meaning that the transmission lines are overloaded, congested and stressed.

Besides overloads due to offline status of system components, transmission lines overloading, congestion and stress can also occur as a result of network concentration between generation and load [7]. Additionally, the mechanical state of facilities is significant for continued power supply while ageing transmission facilities may be strengthened through repairs and replacement of components if there is sufficient evacuation margin of the towers, transformers and conductors to accommodate increase in demand.

Looking at the Nigerian context, one of the major challenges prevalent in our power system is the fact that the

Tele:

E-mail address: god4meks@gmail.com

system thrives on what is being generated at the source in meeting up with the excessive load demand (reactive and active) without adequate compensation. The presence of excessive load in the system without adequate compensation may possibly lead to huge transmission line losses, line congestions, and voltage violations, and a possible operation of the system close to or outside their thermal limits. And under these circumstances, eventual system collapse becomes inevitable.

As system loads vary, the presence of reactive power and its requirements of the transmission system vary expectedly and consequently, increases congestion in the transmission corridor thereby leaving little room for active power flow. Again, excessive demand of reactive power at the load centers introduces $RI^2$and XI^2losses, and consequently, voltage drops, leading to voltage instability of the entire system. Unfortunately, because of inadequate reactive power supply and reserve limits voltage, it may be impractical to meet system power demand through the transmission corridor under such condition [9-10]. Due to these challenges in the transmission lines, the active power generated cannot be effectively transferred to the load centers, and hence, the need for enhancing the loadability of the transmission line. Again, since reactive power cannot be economically and effectively transmitted over long distances, voltage control has to be effected by using special devices (FACTS) dispersed throughout the system [6]. Compensation has to be incorporated manually or automated into the system to guarantee an efficient delivery of real power to the loads independent of the transmission lines and maintain the voltage at the load buses [10].

Reactive power compensation is the generation or absorption of a suitable quantity of capacitive or inductive reactive power to achieve one or more desired effects in an electric power system [16]. These effects include improved voltage profiles, enhanced stability, and increased transmission capacity. Compensation are of two types of compensation exist according to [15]: Load and Line compensation.

1.1 Load Compensation

This is the management of reactive power to improve the quality of supply with respect to the voltage stability and the power factor levels [5], [15]. However, for flat voltage profile under an ideal situation, the reactive power absorbed should be equal to the reactive power generated. But due to losses, the reactive power in the system keeps varying. Therefore, in order to maintain sufficiently flat voltage profile, the reactive power generation is simultaneously controlled or adjusted with respect to an individual load and the compensating device is connected to the load itself [6], [15]. Researchers advocate that transmission network should be designed based on active power transfer capability and the reactive power should be met locally by installing shunt compensating devices (capacitor and inductors) at the point of load where they are needed in order to avoid the extra cost on larger conductors and limit transmission line losses

1.2 Load Compensation

Line compensation involves the use of electrical circuits to modify electrical characteristics of the lines, especially the line length such that its power transfer capacity is enhanced, a near flat voltage profile maintained, and an economical means of reactive power management achieved. Generally, placing series and shunt compensators like capacitors and inductors at suitable locations on the line modify the effective transmission lines impedance; and hence more power can be transferred [18]. This is the principle behind loadability enhancement. The loadability of a transmission line according to [1] is described as the optimum power transfer capability of transmission line under specified set of operating criteria. To operate the power system safely and to gain the benefits of the bulk power transfers, the transfer capabilities must be calculated and the power system planned and operated so that the power transferred do not exceed the transfer capability [9]. Power transfer capability of transmission lines according to [2], are constrained by: thermal limits, voltage drop limits or regulation limit and stability limit.

The work is aimed at enhancing the power transfer capacity of congested power system transmission lines using Static Var Compensator (SVC) and Thyristor Controlled Series Compensator (TCSC). And this achieved with NEPLAN simulator having these set objectives:

(i) To model the 330kV Nigerian Grid of 30 bus in the NEPLAN simulator suitable for load flow studies.

(ii) To identify bus and transmission line states in terms of violations following a load flow study of the test network.

(iii) If transmission line overloads are present, to investigate the impact of TCSC on improving the line loadability of an overloaded line and check its influence on neighboring lines.

(iv) To ascertain the need of and role of the SVC for voltage stability at a bus connecting compensated lines.

(v) Determine the effects of the combined actions of TCSC and a neighboring SVC.

1.3 Review of Related Works

In securing maximum power transfer from the generation station to load buses with acceptable voltage and higher stability level, a number of methods have been proposed by various authors. A review of previous studies on FACTS devices for this purpose reveals that with proper location of the basic FACTS devices, the security, stability and reliability of the power system can be guaranteed to a reasonable extent. Study done by [19] aim to utilize FACTS components such as Fixed Capacitor, Static Synchronous Compensator (STATCOM), and Static VAR Compensator (SVC) in enhancing the voltage stability margin as well as improvement in the power transfer capability in power system. A very effective voltage regulation was also achieved by [10] using STATCOM. They opined that STATCOM is better than SVC in term of performance with an attended smooth profile and lesser harmonic distortion. On the other hand, [21] presented a comprehensive review on the basic principle of operation of Unified Power Flow Control (UPFC), its advantages and performance compared with the various FACTS equipment available. Nisha & Aziz [27] in their work, employed the use of TCSC as a control strategy for power system stability enhancement with focus on TCSC and its role in power system stability enhancement. The use of STATCOM for reactive power support at weak buses to reduce congestion as proposed by [22] helps to increase transmission line loadability and improved voltage profile. In the same way [25] suggested the use of Particle Swarm Optimization (PSO) based algorithm to determine the optimal location and setting of FACTS devices as a way of improving loadability as well as voltage stability and small signal stability. Static VAR Compensator and Thyristor Controlled Series Compensator were used to increase the loadability through the use of Ordinal Optimization Approach [26].

Previous study reveals that a type of FACTS device, UPFC is the most versatile FACT device but for economic

considerations, Thyristor Controlled Series Capacitor (TCSC) has an edge due to its inexpensiveness, simplicity of design and operation [12], [14]. FACTS types in the form of Static Var Compensator (SVC) and the Thyristor-Controlled Series Capacitor (TCSC) were proposed as appropriate for improving voltage stability and transfer capacity of transmission line respectively.

The SVC is predominantly a shunt connected device of variable shunt reactance capable for injecting or absorbing reactive power for voltage regulation and stability. SVC is an automated impedance matching device, designed to bring the system closer to unity power factor. If the power system's reactive load is capacitive (leading), the SVC will use reactors (usually in the form of Thyristor-Controlled Reactors) to consume VARs from the system, lowering the system voltage to nominal. Under inductive (lagging) conditions, the capacitor banks are automatically switched on, thus providing higher system voltage.

TCSC on the other hand, is used in power systems to dynamically control the reactance of a transmission line so as to provide sufficient load compensation [17]. It is a variable impedance device connected in series with the transmission line with the ability to modify the line impedance thereby controlling the power flow through the transmission line. Its presence and operation provides an opportunity to relieve heavily loaded and stressed lines while increasing the transmission corridor or transfer capacity margin so that more power (real) can be transferred through the transmission line.

The works reviewed so far, though quite commendable owing to the fact that all geared towards improving loadability, voltage stability and line losses to a certain degree, it is interesting to note that FACTS devices when operating as series compensators, specializes in improving loadability of a power system network with little or no impact on the voltage stability depending its location in a network, but shunt compensators specializes in voltage stability with little or no impact on loadability depending also on the location in the network. For example, the approach by [22-23] in using STATCOM, a shunt compensator for loadability improvement may not be as efficient as using TCSC, a well-known series compensator for the same purpose. On the other hand, using TCSC as a voltage stability device may not be as efficient as using SVC or STATCOM for the same purpose. Unified Power Flow Controller UPFC being the most versatile device provides both reactive and real power control [14], [21], but it is also the most expensive [14].

In order to truly investigate singular or combined impacts of these devices in the steady state operation of the power grid into which they are incorporated, models that accurately capture their local and neighboring influences on line power flows and bus voltages are indispensable [20].

2 Material and Methods

To achieve the objectives of this study, the following stepwise approaches were implemented with NEPLAN simulation software:

(i) Power system transmission network model was defined. For the purpose of this work, a steady state balanced three-phased model represented by a single-phase model was proposed. The baseline network under review is a 30 Bus Nigeria Interconnected Power System (NIPS).

(ii) Bus admittance matrix of the node voltage equation was formed.

(iii) Load flow equations for the baseline NIPS 30 – Bus Network were formed.

(iv) Load flow simulation was carried out with the formulated equations in a NEPLAN environment to determine the bus voltage magnitudes, power flows and line losses on the lines for the baseline NIPS 30 – Bus Network.

(v) The TCSC/SVC mathematical model for power flow/voltage regulation is formed.

(vi) The formulated TCSC/SVC model was incorporated into the load flow equations model.

(vii) Simulation of the entire model was then carried out with NEPLAN to investigate the impact of the TCSC/SVC on the transmission line and at the buses.

(viii) TCSC is activated at overloaded lines and SVC at the buses with voltage limit violation. This is to verify the effects of the combined and separate actions of a TCSC and or a neighboring SVC. This can be achieved by exploring these three options:

(a) Activating TCSC, while SVC is deactivated.

(b) Deactivating TCSC while SVC is active, and

(c) Activating both TCSC and SVC

3. Theory/Calculation

3.1 Maximum Power Transfer of Transmission Line

The flow of active power (P) and reactive power (Q) through transmission system has influence on voltage magnitude and phase difference of voltage at terminals and voltage along the line [2]. The receiving-end powers according to [3], [13] are as follows:

$$\boldsymbol{P_R = \frac{|V_S||V_R|}{|Z|}\cos(\theta-\delta) - \frac{|V_R|^2}{|Z|}\cos\theta} \quad (1)$$

Where, $\boldsymbol{\alpha = 0}$, $\boldsymbol{\beta = \theta}$, for short lines.

$$\boldsymbol{Q_R = \frac{|V_S||V_R|}{|Z|}\sin(\theta-\delta) - \frac{|V_R|^2}{|Z|}\sin\theta} \quad (2)$$

Similarly, sending-end powers are:

$$\boldsymbol{P_S = \frac{|V_S|^2}{|Z|}\cos\theta - \frac{|V_S||V_R|}{|Z|}\cos(\theta+\delta)} \quad (3)$$

$$\boldsymbol{Q_S = \frac{|V_S|^2}{|Z|}\sin\theta - \frac{|V_S||V_R|}{|Z|}\sin(\theta+\delta)} \quad (4)$$

where

$\boldsymbol{P_R}$, $\boldsymbol{Q_R}$ and $\boldsymbol{V_R}$ are the receiving end active power, reactive power and bus voltage while $\boldsymbol{P_S}$, $\boldsymbol{Q_S}$ and $\boldsymbol{V_S}$ are the sending end counterparts respectively. The transmission line resistance, reactance and impedance are $\boldsymbol{R}$, $\boldsymbol{X}$ and $\boldsymbol{Z}$ respectively.

The receiving-end power (power transferred) is maximum when $\boldsymbol{\delta = \theta}$.

From equation (1) with $\boldsymbol{\cos\theta = \frac{R}{Z}}$

$$\boldsymbol{P_R(max) = \frac{|V_S V_R|}{|Z|} - \frac{|V_R|^2}{|Z|}\cos\theta}$$

$$\boldsymbol{P_R(max) = \frac{|V_S V_R|}{|Z|} - \left[\frac{|V_R|}{|Z|}\right]^2 R} \quad (5)$$

Since $\boldsymbol{R \ll X}$, then $\boldsymbol{Z \approx X}$

$$\boldsymbol{\therefore \theta = \tan^{-1}\left(\frac{X}{R}\right) \approx 90^0}$$

From equations (1) and (2), the receiving-end powers $\boldsymbol{P_R}$ and $\boldsymbol{Q_R}$ is:

$$\boldsymbol{P_R = \frac{|V_S||V_R|}{X}\sin\delta} \quad (6)$$

$$\boldsymbol{Q_R = \frac{|V_S||V_R|}{X}\cos\delta - \frac{|V_R|^2}{X}} \quad (7)$$

where δ is the phase, torque or load angle between sending and receiving-end voltages.

As observed from equation (6), the power transferred over a transmission line is inversely proportional to the inductive reactance of the system. Implying that the reactance of a transmission line sets the limit on the maximum power

that can be transmitted by a line for a given transmission voltage with respect to the power angle.

According to [15], it was also observed from the above equation that:

(i) When the resistance of a transmission line is negligibly small, i.e. zero, the active power transmitted through the transmission line is proportional to the $\boldsymbol{sin\delta = \delta}$ $\boldsymbol{(for\ small\ value\ of\ \delta)}$, and the reactive power is proportional to the voltage drops across the line.

(ii) The active power received is maximum, $\boldsymbol{P_{max}}$ when $\boldsymbol{\delta = 90^0}$ and has a value of $\frac{|V_S||V_R|}{X_L}$. However, the value of $\boldsymbol{\delta}$ is always kept less than $\boldsymbol{90^0}$ for stability considerations.

(iii) Maximum active power transfer over the line can be obtained by raising the excitation of the system or by reducing reactance of the line.

And to ensure adequate stability margin, the practical operating load angle is usually limited to $\boldsymbol{35^0}$ to $\boldsymbol{45^0}$. When there is a sudden change in transmission system, like a change in load, tripping of generator or load, sudden switching of load, any fault etc., it will result in oscillation in the load angle δ. If load angle δ goes beyond $\boldsymbol{90^0}$, the synchronism is lost and the transmission system fails to transfer the power [3-4].

3.2 Model for Reactive Power Flow with SVC

Figure1 shows a shunt connection of the SVC module showing direction of flow of reactive power $\boldsymbol{Q_{SVC}}$ in/out of bus $\boldsymbol{i}$. It is made up of a fixed capacitor (FC) with a reactance $\boldsymbol{X_C}$ and a thyristor controlled reactor (TCR) whose reactance is a function of the thyristor firing angle α.

The thyristor controlled reactor's equivalent reactance $(\boldsymbol{X_{TCR}(\alpha)})$ is given by:

$$\boldsymbol{X_{TCR}(\alpha) = \frac{\pi X_L}{\sigma - \sin\sigma}} \quad (8)$$

Where the conduction angle, $\boldsymbol{\sigma = 2(\pi - \alpha)}$, and the inductive reactance, $\boldsymbol{X_L = \omega L}$; and substituting,

$$\boldsymbol{X_{TCR}(\alpha) = \frac{\pi X_L}{2(\pi-\alpha)+\sin(2\alpha)}} \quad (9)$$

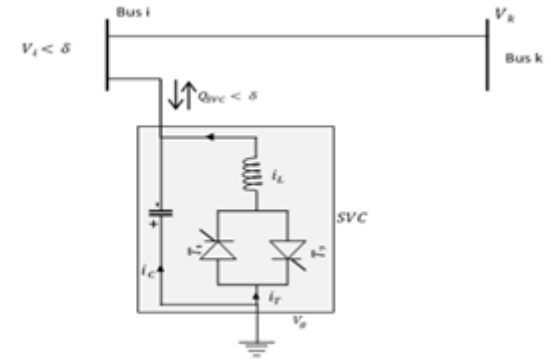

Fig. 1. Schematic diagram of the SVC implemented in shunt connection to bus.

The effective reactance of SVC, $\boldsymbol{X_{svc}(\alpha)}$ is determined by the parallel combination of a thyristor controlled reactor equivalent reactance $(\boldsymbol{X_{TCR}(\alpha)})$ and a fixed capacitive reactance $(\boldsymbol{X_C})$.

$$\boldsymbol{\frac{1}{X_{svc}(\alpha)} = \frac{1}{X_C} + \frac{1}{X_{TCR}(\alpha)}} \quad (10)$$

$$\boldsymbol{X_{svc}(\alpha) = \frac{X_C X_{TCR}(\alpha)}{X_C + X_{TCR}(\alpha)}}$$

$$\boldsymbol{X_{svc}(\alpha) = \frac{\pi X_C X_L}{X_C[2(\pi-\alpha)+\sin 2\alpha] - \pi X_L}} \quad (11)$$

Given that the equivalent impedance $\mathbf{Z}_{svc}$ of the *SVC* is

$$\mathbf{Z}_{svc} = \mathbf{R}_{svc} + j\mathbf{X}_{svc}(\alpha) \quad (12)$$

This implies that the equivalent admittance is

$$\mathbf{Y}_{svc} = \frac{1}{\mathbf{Z}_{svc}} = \mathbf{G}_{svc} + j\mathbf{B}_{svc} \quad (13)$$

where, $\mathbf{G}_{svc}$ and $\mathbf{B}_{svc}$ is the equivalent conductance and susceptance of SVC respectively.

By complex conjugate,

$$\frac{1}{R_{svc}+jX_{svc}} = \frac{R_{svc}-jX_{svc}}{(R_{svc}+jX_{svc})(R_{svc}-jX_{svc})}$$

Further manipulation with $\boldsymbol{R_{svc} = 0 \implies G_{svc} = 0}$ yeilds

$$\mathbf{G}_{svc} + j\mathbf{B}_{svc} = \frac{R_{svc}}{(R_{svc}{}^2 + X_{svc}{}^2)} - j\frac{X_{svc}}{(R_{svc}{}^2 + X_{svc}{}^2)} \quad (14)$$

And from (13)

$$\mathbf{B}_{svc} = -\frac{X_{svc}}{X_{svc}{}^2} = -\frac{1}{X_{svc}} \quad (15)$$

Meaning that the equivalent susceptance of the device $\mathbf{B}_{svc}$ is the negative inverse of the equivalent reactance $\mathbf{X}_{svc}$, and from (11)

$$\mathbf{B}_{svc} = -\mathbf{1}/\frac{\pi \mathbf{X_C X_L}}{\mathbf{X_C}[2(\pi-\alpha)+\sin 2\alpha] - \pi \mathbf{X_L}}$$

$$\mathbf{B}_{svc} = -\frac{\mathbf{X_C}[2(\pi-\alpha)+\sin 2\alpha] - \pi \mathbf{X_L}}{\pi \mathbf{X_C X_L}}$$

$$\mathbf{B}_{svc} = \frac{-[2(\pi-\alpha)+\sin 2\alpha]}{\pi \mathbf{X_L}} + \frac{1}{\mathbf{X_C}} \quad (16)$$

For a plot of *B* (susceptance) against firing angle α, the resonance angle, $\boldsymbol{\alpha_{res} = 115^0}$, corresponds to the zero crossing of the plot with the values of $\mathbf{X_L}$ and $\mathbf{X_C}$ chosen as 0.1134Ω and 0.2267Ω respectively and $\mathbf{X_{TCR} = X_C}$ and $\mathbf{X_{SVC} = B_{SVC} = 0}$. At the condition $\boldsymbol{90^0 < \alpha < \alpha_{res}}$, the circuit is in the capacitive boost mode as $\mathbf{X_{svc}}$ is negative corresponding to capacitive reactance behavior. At condition $\boldsymbol{\alpha = 90^0}$, the device operates in a blocking mode. The thyristor is not triggered and hence is non-conducting. At condition $\boldsymbol{\alpha_{res} < \alpha < 180^0}$, the device is in the inductive boast mode as $\mathbf{X}_{svc}$ is positive corresponding to inductive reactance behavior.

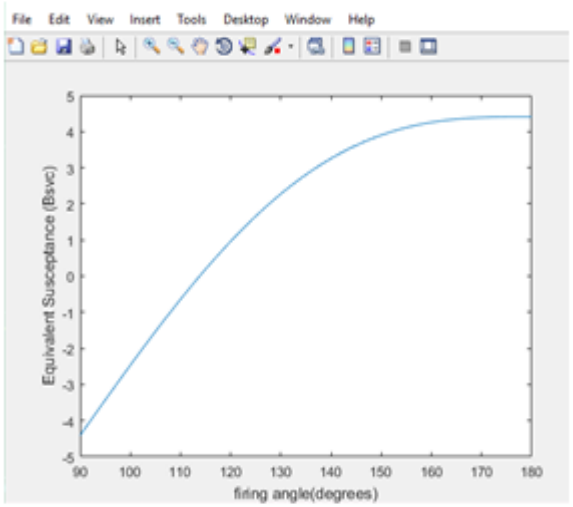

Figure 2. SVC Equivalent Susceptance Profile.

With $\boldsymbol{B_{svc}^{min} \le B_{svc}(\alpha) \le B_{svc}^{max}}$, the power that flows from bus $\boldsymbol{i}$ to the SVC is

$$\boldsymbol{S_{svc} = V_i V_i{}^* Y_{svc}{}^* = P_{svc} + jQ_{svc}}$$
$$\boldsymbol{= |V_i|\angle\delta_i |V_i|\angle -\delta_i |Y_{svc}|\angle -\delta_{svc}}$$
$$\boldsymbol{= |V_i|^2 |Y_{svc}|\angle(\delta_i - \delta_i - \delta_{svc})}$$

$$\boldsymbol{S_{svc} = |V_i|^2 |Y_{svc}|\angle(-\delta_{svc})} \quad (17)$$

$$\boldsymbol{Q_{svc} = -|V_i|^2 B_{svc}} \quad (18)$$

Substituting (16) in (18);

$$\boldsymbol{Q_{svc} = |V_i|^2 \left[\frac{[2(\pi-\alpha)+\sin 2\alpha]}{X_L} - \frac{1}{X_C}\right]} \quad (19)$$

This is the reactive power injected or absorbed from the bus by the SVC.

3.3 Mathematical Model for Reactive Power Flow with TCSC

Figure 3 shows the TCSC module connected in series with the transmission line. The equivalent reactance of the TCSC at 50 Hz is rather represented with a steady state total current instead of a steady state voltage. In this study, TCSC is represented by its fundamental frequency impedance. The TCSC linearized power flow equations, with respect to the firing angle, are incorporated into an existing Newton-Raphson algorithm for load flow analysis.

The equivalent reactance of TCSC with respect to the firing angle α, $\boldsymbol{X_{TCSC}(\alpha)}$ is given by [8] as:

$$\boldsymbol{X_{TCSC}(\alpha) = X_C - B_1(X_C + B_2) - B_4 B_5} \quad (20)$$

Where; $\boldsymbol{B_1 = [2(\pi-\alpha) + \sin 2(\pi-\alpha)]/\pi}$,

$\boldsymbol{B_2 = \frac{X_C X_L}{X_C + X_L}}$, $\boldsymbol{B_3 = \sqrt{\frac{X_C}{X_L}}}$,

$\boldsymbol{B_4 = B_3 \tan[B_3(\pi-\alpha)] - \tan(\pi-\alpha)}$,

$\boldsymbol{B_5 = 4B_2^2 \cos^2(\pi-\alpha)}$ and $\boldsymbol{X_C = \frac{1}{2\pi f C}}$;

Subsequent substitution yields

$$X_c - \left[\frac{2(\pi-\alpha)+\sin 2(\pi-\alpha)}{\pi}\right]\left[X_c + \frac{X_c X_L}{X_c - X_L}\right] - \left[\sqrt{\frac{X_c}{X_L}}\tan\left(\sqrt{\frac{X_c}{X_L}}(\pi-\alpha)\right) - \tan(\pi-\alpha)\right]\left(4\left(\frac{X_c X_L}{X_c - X_L}\right)^2 \cos^2(\pi-\alpha)\right) \quad (21)$$

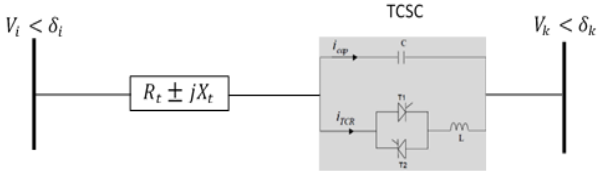

Fig.3. TCSC module connected in series with line impedance

The number of resonant points has great influence over the behavior of TCSC power flow model. This number is given by

$\boldsymbol{\alpha = \pi\left[1 - \frac{(2n-1)\omega\sqrt{LC}}{2}\right]}$; where, n = 1, 2, 3….

A plot of the equivalent reactance of the TCSC as a function of the firing angle in the range of 90-180° using $\boldsymbol{X_C = 0.2267}$ and $\boldsymbol{X_C = 0.11}$ is shown in Fig.3

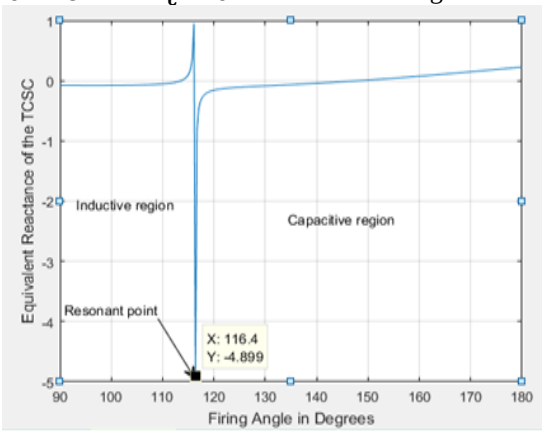

Fig.4. Resonant Point Impedance Characteristic Curve.

The TCSC has two operating ranges around its internal circuit resonance: first is $\boldsymbol{\alpha_{Clim} \le \alpha \le 180^0}$;where $\boldsymbol{X_{TCSC}(\alpha)}$ is capacitive and the second is $\boldsymbol{90^0 \le \alpha \le \alpha_{Llim}}$, where $\boldsymbol{X_{TCSC}(\alpha)}$ is inductive.

As shown in Figure 4, the resonant point exists at 116.4^0 at TCSC reactance of -4.90Ω.

The expression for the TCSC power flow equation from bus $\boldsymbol{i}$ to $\boldsymbol{k}$, $\boldsymbol{S_{ik}}$ is given by:

$$\boldsymbol{S_{ik} = V_i I_{ik}^* = V_i Y_{ik}^* (V_i^* - V_k^*)} \quad (22)$$

But

$$\boldsymbol{Y_{ik}^* = \frac{1}{R_{ik} + j(X_{ik} \pm X_{TCSC})} = \frac{R_{ik} - j(X_{ik} \pm X_{TCSC})}{R_{ik}^2 + (X_{ik} \pm X_{TCSC})^2}}$$

$$\boldsymbol{Y_{ik}^* = G_{ik} - jB_{ik}} \quad (23)$$

where,

$\boldsymbol{G_{ik} = \frac{R_{ik}}{R_{ik}^2 + (X_{ik} \pm X_{TCSC})^2}}$ and

$\boldsymbol{B_{ik} = -j\frac{R_{ik} - j(X_{ik} \pm X_{TCSC})}{R_{ik}^2 + (X_{ik} \pm X_{TCSC})^2}}$

From (22),

$$\boldsymbol{V_i(V_i^* - V_k^*) = V_i^2 - V_i V_k e^{j\delta_{ik}}} \quad (24)$$

where $\boldsymbol{\delta_{ik} = \delta_i - \delta_k}$; and substituting (24) and (23) in (22)

$$\boldsymbol{S_{ik} = V_i^2(G_{ik} - jB_{ik}) - V_i V_k(G_{ik} - jB_{ik})(\cos\delta_{ik} + j\sin\delta_{ik})} \quad (25)$$

Separating the imaginary component from the real component from (25) implies that:

$$\boldsymbol{P_{ik} = V_i^2 G_{ik} - V_i V_k(G_{ik}\cos\delta_{ik} + B_{ik}\sin\delta_{ik})} \quad (26)$$

$$\boldsymbol{Q_{ik} = -V_i^2 B_{ik} - V_i V_k(G_{ik}\sin\delta_{ik} - B_{ik}\cos\delta_{ik})} \quad (27)$$

3.4 Implementation of NIPS – 30 Bus Network

For validation of this work, various stages of simulations were carried out on the Nigeria Interconnected Power Systems (NIPS) 30 Bus Network using NEPLAN

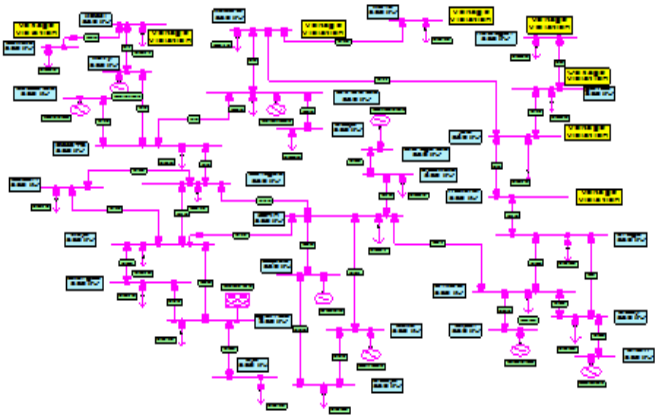

Fig.5. Baseline Load Flow Simulation of NIPS 30 Bus Network. .

Figure 5 is a baseline load flow analysis of Nigerian Electric Power Interconnected Power System network at 330kV using NEPLAN without the compensating actions of TCSC and SVC which converged after 6 iteration using Newton Raphson method. The buses marked with yellow indicate elements overload and voltage violations. The variants of this figure represent the one-line diagram with either the TCSC or SVC switched on while the other is off. The essence of this analysis is to ascertain possible transmission line overloads and violations in terms of bus voltage magnitude.

3.5 Location of TCSC in the Network Using P-V Curve

The placement of TCSC was done using P-V curve in voltage stability analysis as shown in Fig. 6. P-V curve is used to establish the relationship between the bus voltages and load within a specified region. It provides information on the nearness to voltage collapse as the load level increases. So the bus with the lowest percentage of voltage profile contributes most to collapse in the event of overloading. From the graph, the choice of placement of TCSC is considered ideal between the two critical points of voltage collapse: Makurdi bus and Jos bus. Also Enugu and Onitsha bus is the next suitable.

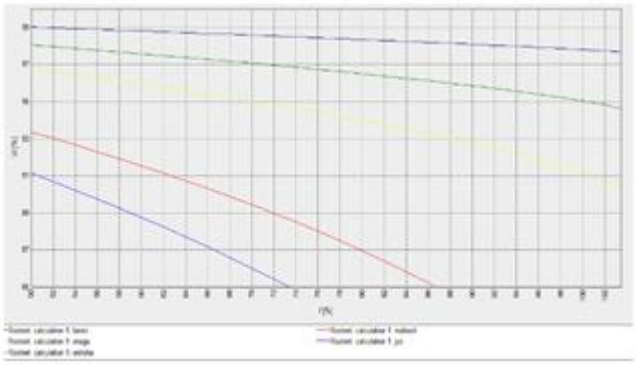

Fig.6. P-V Curve.

3.6 Location of SVC in the Network Using Q-V curve

The placement of SVC was done using Q-V curve in voltage stability analysis method. This method was used to identify the weakest point (buses) of the system network. The weakest bus here is one that has the least reactive power support, and lowest reactive power margin. The minimum point of a Q-V curve is the critical point. From the Q-V curve in Figure 7, the region above the horizontal line establishes the need to inject reactive power at Sokoto bus station because it has the least reactive power support, while at the region below horizontal line, Kano bus station has the least reactive power support followed by Jos bus station. Therefore, three nodes (Kano, Sokoto, and Jos Stations) are ideal for reactive power compensation.

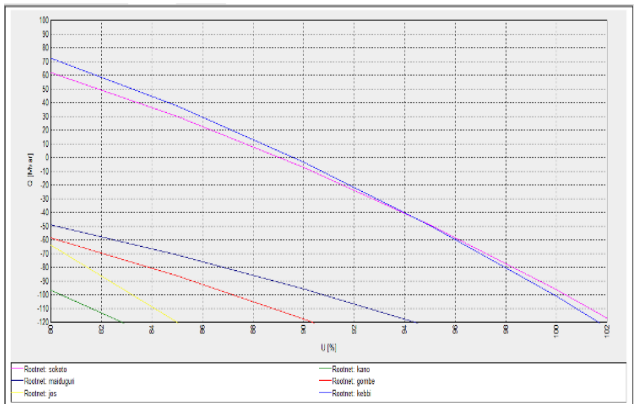

Fig.7. Q-V curve .

4. Results and Discussion

4.1 Baseline Analysis of the Network

A load flow nodal analysis conducted with NEPLAN on the baseline network shows that the system was overloaded at Gombe, Jos, Kaduna, Kano, Kebbi, Maiduguri, Makurdi, and Sokoto bus station, with a consequent lower voltage violation as shown in Fig.8 indicated by the point of red patch along the curve.

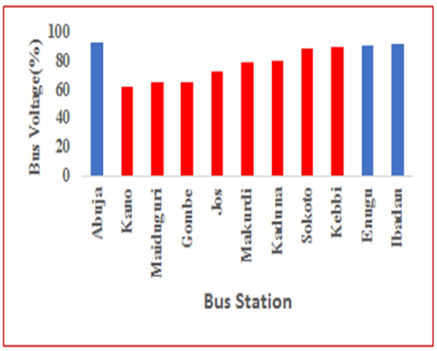

Fig.8. Baseline chart obtained from Load Flow Nodal Analysis of NIPS Network.

The reason for this violation is because the minimum (%) and maximum (%) nominal voltage for all the nodes except node 1 (slack bus) was set at 90% and 110% of the different reference bus voltages respectively. For example, Fig.8 shows that at Gombe bus station, the percentage voltage profile level of 65.77% is below the 90% minimum set reference; indicating low voltage violation. The same is the case at Kano, Maiduguri, Jos, Makurdi, Kaduna, Sokoto, and Kebbi, with 62.29%, 65.37%, 72.83%, 79.48, 89.07, and 89.63% respectively.

Figure 9 shows the total active and reactive power loss in the network at baseline (before intervention).

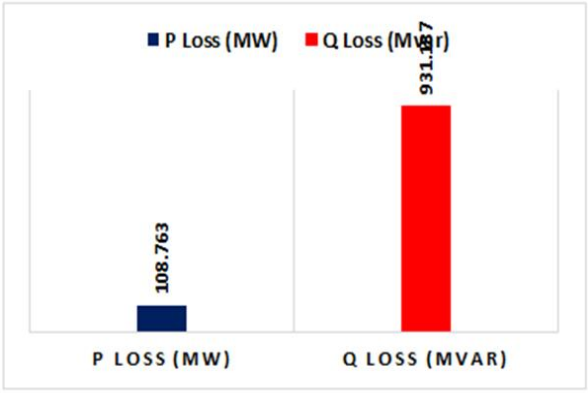

Figure 9. Chart of Total Active and Reactive Line Losses in the Network at Baseline.

4.2 Impact of TCSC with respect to Loadability.

The result of the load flow analysis as shown in data generated the Table 1 and chart in Fig.10 showed that the power transfer capacity (loadability) of the transmission line L6 (Jos-Makurdi) was significantly improved from 221.602MW to 289.466MW, with improved capacity margin of about 68 MW (about 31%) for more active power flow on the line. Also on L34 (between Onitsha and Enugu), active power transfer capacity was greatly improved from 184.763MW to 294.021MW, with improved caacity margin of about 109 MW (about 60%).

There was also significant improvement on the active power transfer capacity for some of the transmission lines sharing the same node/bus with line L6 and line L34. For instance, the active power on line L11 (Jos-Kaduna) increased from 45.497MW to 121.307MW with capacity margin of about 76MW (about 167%). Also in line L19 (Markudi-Enugu), active power transfer capacity was enhanced from 229.118MW to 300.754MW; about 72MW capacity margin (31%). Onitsha-Okpai line (L22) also witnessed increased active power transfer capacity.

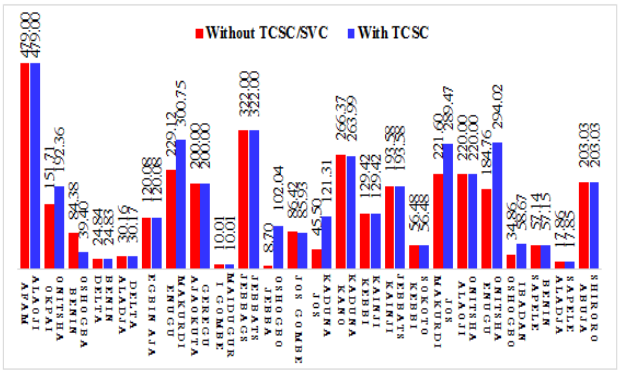

Figure 10. Load Flow Analysis of Lines for Loadability Enhancement with and without TCSC.

Table 1. Load Flow Data Generated before and after the three Interventions.

Element Name	Without TCSC/SVC		With TCSC		With SVC		With TCSC & SVC	
	P (MW)	Q (Mvar)	P (MW)	Q (Mvar)	P (MW)	Q (Mvar)	P (MW)	Q (Mvar)
L23	479.00	266.62	479.00	241.05	479.00	180.16	479.00	154.63
L18	136.70	25.00	136.70	26.38	136.70	20.52	136.70	19.84
L28	55.47	-2.07	46.89	-1.61	41.83	-2.64	38.30	-2.78
L22	151.71	67.00	192.36	86.45	147.39	38.02	192.18	34.57
L9	161.60	100.95	121.03	56.56	166.15	45.36	121.40	23.69
L29	84.38	33.57	39.40	34.99	66.32	36.10	29.94	39.41
L21	52.17	-68.47	17.83	79.20	35.29	-35.09	25.08	25.34
L31	24.84	72.52	24.83	75.25	24.88	63.60	24.89	62.25
L32	30.16	16.61	30.17	16.61	30.12	16.62	30.11	16.62
L24	468.40	230.99	452.39	229.15	442.95	225.56	436.37	224.20
L27	292.55	148.88	283.78	147.77	278.60	145.72	274.99	144.92
L26	120.08	62.26	120.08	62.26	120.08	62.26	120.08	62.26
L19	229.12	139.61	300.75	158.84	247.68	-5.53	309.55	-31.33
L33	200.00	58.04	200.00	59.42	200.00	53.55	200.00	52.87
L4	10.01	5.23	10.01	5.20	10.01	5.17	10.01	5.17
L17	23.48	44.39	1.33	-43.83	25.09	46.70	1.25	49.54
L15	63.88	-1.80	39.07	-0.04	45.15	-0.92	27.99	0.79
L16	143.22	45.92	119.16	46.75	125.03	46.09	108.41	47.15
L13	322.00	146.69	322.00	120.44	322.00	128.35	322.00	112.32
L5	497.99	29.23	404.67	9.02	444.72	16.94	374.38	3.93
L3	8.70	101.47	102.04	93.02	63.18	93.54	133.53	89.04
L12	86.42	59.94	85.93	55.72	85.41	51.27	85.41	51.27
L11	45.50	-91.08	121.31	-35.96	68.37	37.76	132.97	33.27
L10	266.37	248.24	263.99	227.93	257.40	-54.18	257.39	-53.40
L1	129.42	104.31	129.42	104.31	128.22	2.74	128.22	2.74
L2	193.58	0.06	193.58	-2.52	194.78	-1.83	194.78	-3.41
L36	56.48	42.91	56.48	42.91	56.47	-48.32	56.47	-48.32
L6	221.60	75.05	289.47	61.89	241.82	-55.84	300.61	-108.09
L42	220.00	103.18	220.00	121.77	220.00	63.00	220.00	58.47
L34	184.76	135.44	294.02	172.33	197.87	37.61	302.26	13.21
L14	34.86	56.70	58.67	53.73	52.84	54.80	69.34	52.69
L20	57.14	150.73	57.15	156.45	57.10	132.06	57.09	129.23
L30	17.86	8.17	17.85	8.17	17.90	8.16	17.91	8.16
L8	443.94	660.37	357.96	518.74	395.06	84.25	329.70	83.30
L35	203.03	128.27	203.03	128.27	203.03	128.27	203.03	128.27

4.3 Impact of TCSC on Transmission Lines' Losses.

Summary of load flow analysis on the entire network when only TCSC was activated revealed that there was a significant reduction in active power line loss from 108.763MW to 83.988MW and reactive power line loss from 931.187Mvar to 717.803Mvar as shown in Fig.11

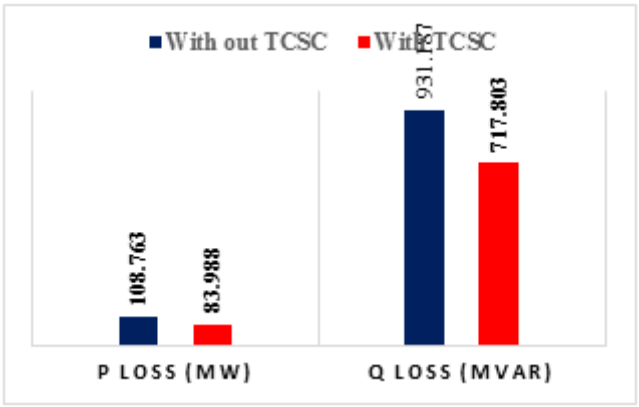

Figure 11. Chart of Total Active and Reactive Line Losses in the Network with and without TCSC.

4.4 Impact of TCSC and SVC with Respect to Loadability

Figure 12 is the proposed solution for loadability enhancement voltage stability in NEPLAN view of the NIPS 30 bus network with both TCSC and SVC incorporated. As stated earlier, TCSC were installed in-between Jos & Makurdi, and in-between Enugu & Onitsha, and SVC at Jos, Kano and Sokoto bus stations.

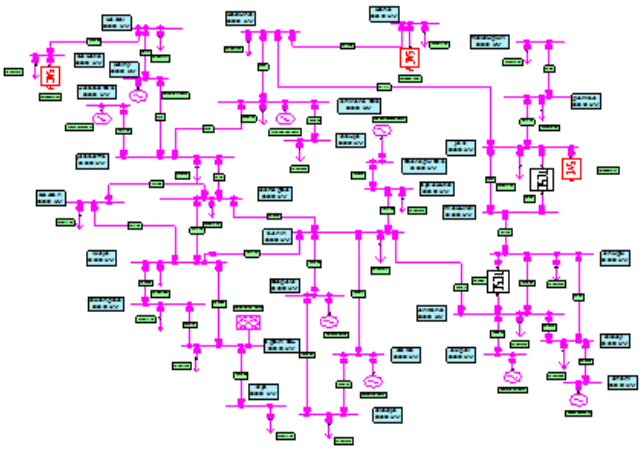

Fig.12. Proposed Solution for Loadability Enhancement voltage stability in NEPLAN view for the NIPS 30 Bus Network with both TCSC and SVC Incorporated.

Figure 13 is the load flow chart showing loadability at baseline and at the three interventions drawn from the data generated on load flow in Table 1. The result shows that the power transfer capacity (loadability) of the transmission line L6 (Jos-Makurdi) was significantly improved from

221.602MW to 289.466MW when only TCSC was activated, with improved capacity margin of about 68 MW (about 31%) for more active power flow on the line as compared to 300.61MW when both TCSC and SVC were activated (about 35% improved capacity margin). Both values were quite more pronounced compared to 241.82MW obtained when only SVC was activated. The same thing played out at Onitsha–Enugu transmission line. Upon activation of only TCSC, the active power transfer of 294.02MW (with improved capacity margin of about 109 MW (about 60%) with respect to baseline of 184.763MW) was recorded as compared to 302.26MW (about 64%) recorded when both TCSC and SVC were activated. The neighboring lines that shares the same node with the line L6 and line L34 (Onitsha-Enugu) where TCSC were located also had some significant impact. For example, at transmission line L11 (Kaduna-Jos), the active power transfer capacity when only TCSC was activated was 121.31MW as compared to 132.97MW when both TCSC and SVC were activated; about 192% compared to the baseline (no intervention). Both values were quite more pronounced compared to 68.37MW obtained when only SVC was activated with 45.50MW at baseline. This means that there was slight improvement on the power transferred when only SVC was activated compared to the baseline.

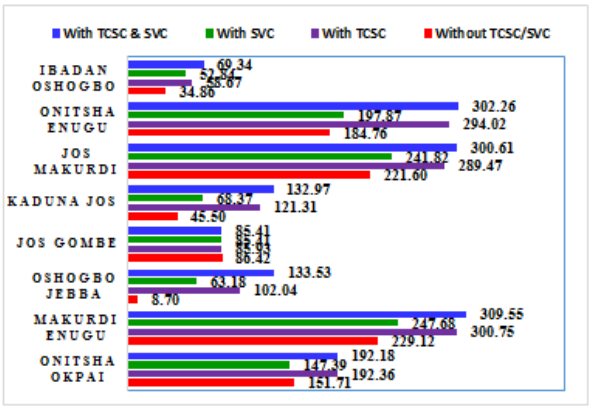

Figure 13. Load flow chart showing loadability at baseline and the three interventions.

4.5. Impact of TCSC and SVC with Respect to Line Losses

Summary of load flow analysis on the entire network as shown in Fig.14 reveals that active power loss decreased from 108.763MW to 83.98MW with the presence of TCSC (about 23% reduction) with a consequent reduction in reactive power loss from 931.187Mvar to 717.803Mvar.

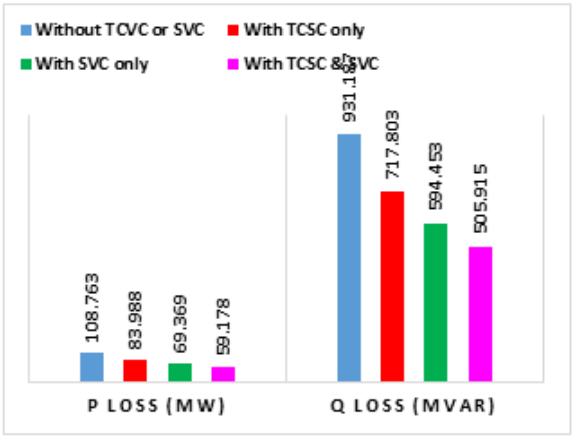

Figure 14. Load flow chart showing line losses at baseline and the three interventions.

There was further reduction of active and reactive power to 69.369MW and 594.453MW respectively when only SVC was activated. With the presence of both TCSC and SVC, total active power loss with respect to the baseline of 108.763MW was reduced to 59.178MW (about 46% reduction). Also total reactive power loss was reduced from the baseline of 931.187Mvar to 505.915Mvar (also about 46% reduction).

4.6 Impact of TCSC and SVC with Respect to Voltage Stability.

Figure 15 is the result of the nodal analysis of the entire network drawn from the table in Appendix B. It shows the state of the entire network before and after intervention. Before intervention, voltage violations occurred at Gombe, Jos, Kaduna, Kano, Kebbi, Maiduguri, Makurdi, and Sokoto bus stations with percentage bus voltage profile of 65.77%, 72.83%, 79.96%, 62.29%, 89.63%, 65.37%, 79.46%, and 89.07% respectively. With the presence of TCSC in-between Jos and Makurdi bus stations, the changes in voltage profile were not significant in the sense that the percentage bus voltage profiles were still below the set or reference point of 90%. Hence, there were still violations at those nodes earlier mentioned. But when only SVC was activated at Sokoto, Kano, and Jos bus station, there were significant boost in the voltage profile with percentage bus voltage profile of 94.83%, 99.50%, 96.84%, 99.50%, 99.09%, 94.55%, 95.48%, and 99.50% for Gombe, Jos, Kaduna, Kano, Kebbi, Maiduguri, Makurdi, and Sokoto bus stations respectively. Also with the combined presence of TCSC & SVC at the locations mentioned previously, apart from Kaduna and Makurdi bus station with 98.89% and 99.50% percentage bus voltage profile respectively, the rest of the stations have the same voltage profile when only SVC was activated.

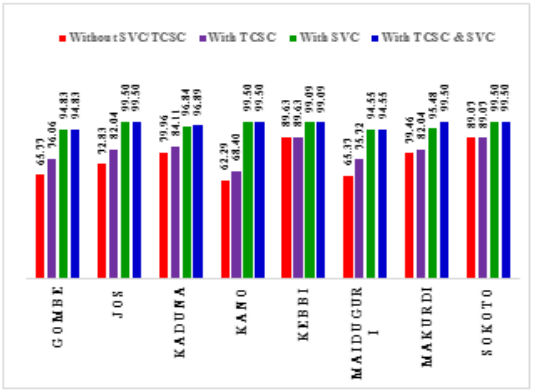

Figure 15. Load flow nodal analysis chart showing percentage voltage profile of buses at baseline and the three interventions.

Conclusion

Findings from this work shows that transmission line loadability can be greatly enhanced using combined effect of a series and a shunt compensator. This work employed the services of TCSC – a series compensator and SVC – shunt compensator. The impact of TCSC and SVC on a congested overloaded transmission line was investigated by simulation using NEPLAN and the result reveals that:

(i)The presence of TCSC in-between two nodes of a transmission line actually enhanced active power transfer capacity of that line; i.e., the ability of that line to deliver active power effectively to the load thereby causing a relief to the overloaded lines.

(ii)Adding TCSC on a line influences the neighboring lines sharing the same node with the line on which it was incorporated in terms of improved loadability, reduction in power losses.

(iii)The congestion problem caused by overload and the presence of reactive component was effectively reduced by introducing TCSC on the lines and SVC at the buses.

(iv)The presence of SVC and TCSC effectively combined and coordinated, enhanced the voltage profile as well as its power system stability. However, it was observed that uncoordinated positioning of TCSC on a line causes either lower or upper voltage violation at the nodes connecting the line. The answer was found in the use of Q-V and P-V curve from voltage stability analysis for proper positioning of TCSC and SVC.

(v)It is worthy of note here that the main reason for the combined services of TCSC and SVC is such that the TCSC complements the deficiency of SVC's its inability to enhance loadability, while the SVC complements TCSC's inability to improve on the voltage profile.

Conflicts of interest: none

Funding: This research did not receive any specific grant from funding agencies in the public, commercial, or not-for-profit sectors.

Acknowledgment

We acknowledge the role of the co-authors towards making the research work worthwhile and then the management of Electronic Development Institute for providing an enabling environment for the study.

Author Biographies

Author 1 Okwuelu Nnameka holds his B.Eng in Electrical Electronics Engineering in University of Agriculture, Makurdi, and M.Eng. in Power System Engineering at Enugu State University of Science and Technology, Nigeria. He presently works in the Research and Development Department of Electronics Development Institute, Awka, Anambra State, Nigeria. He is a registered member of COREN and his research interest is in Power System and Power Electronics Engineering. He can be reached via god4meks@gmail.com

Author 2 Onyedikachi Samuel holds a B. Eng and M.Eng in Electrical Electronics Engineering and is a lecturer with the department of Electrical Engineering at Nnamdi Azikiwe University, Awka, Anambra State of Nigeria. His Research interests are in Power System Operation and Contrrol Reliability studies, Renewable Energy Integration and Optimization techniques in Power System.

Author 3 Udeze Chidiebele .C. received his B. Eng in Electrical and Electronics Engineering; his M.Sc, and Ph.D in Computer and Control Systems Engineering all from Nnamdi Azikiwe University Awka, Anambra State, Nigeria. He is a Lecturer in Electronic Engineering Department, University of Nigeria Nsukka. He is a COREN registered Engineer and a member of Nigerian Society of Engineers. His current research interest includes: Control Systems Engineering, Artificial Intelligence and Robotics, Cloud Computing and Applications, Internet of Things.

E-mail: chidiebele.udeze@unn.edu.ng

References

1. Chakrabarti, A., & Halder, S. (2010). Power System Analysis: Operation And Control 3Rd Ed: PHI Learning Pvt. Ltd.
2. Bakshi, U., & Bakshi, M. (2009). Generation, transmission and distribution: Technical Publications.
3. Gonen, T. (2011). Electrical power transmission system engineering: analysis and design: CRC Press.
4. Saadat, H. (1999). Power system analysis: WCB/McGraw-Hill.
5. Kothari, D. P., & Nagrath, I. (2003). Modern power system analysis: Tata McGraw-Hill Education.
6. Kundur, P., Balu, N. J., & Lauby, M. G. (1994). Power system stability and control (Vol. 7): McGraw-hill New York.
7. Yao, L., Cartwright, P., Schmitt, L., & Zhang, X.-P. (2005). Congestion management of transmission systems using FACTS. Paper presented at the Transmission and Distribution Conference and Exhibition: Asia and Pacific, 2005 IEEE/PES.
8. Panda, S., Padhy, N., & Patel, R. (2007). Modelling, simulation and optimal tuning of TCSC controller. International Journal of Simulation Modelling, 6(1), 37-48.
9. Dugan, R. C., McGranaghan, M. F., & Beaty, H. W. (1996). Electrical power systems quality. New York, NY: McGraw-Hill,| c1996.
10. Rudrangshu, C., Soham, C., Sourojit, M., Rajarshee, R. C., Rijoy, C., Shukti, S. M., & Shuvam, H. (2015). Comparative Analysis of STATCOM and SVC Operation in Electric Transmission Line. International Journal of Emerging Technology and Advanced Engineering, 5(8), 323-329.
11. Schlabbach, J., & Rofalski, K.-H. (2008). Power system engineering: planning, design, and operation of power systems and equipment: John Wiley & Sons.
12. Schaffner, C., & Anderson, G. (2001). Use of facts devices for congestion management in a liberalized market. Swiss Federal Institute of Technology (ETH), Zurich, Tech. Rep.
13. Sivanagaraju, S. (2008). Electric power transmission and distribution: Pearson Education India.
14. Song, Y.-H., & Johns, A. (1999). Flexible ac transmission systems (FACTS): IET.
15. Wadhwa, C. (2006). Electrical power systems: New Age International.
16. Whitaker, J. C. (2006). AC power systems handbook: CRC Press.
17. Yu, J. (2009). FACTS: Thyristor-Controlled Series Compensation. Jawnsy's Journal on Life, Software and Engineering. Jawnsy's Journal on Life, Software and Engineering.
18. Yukseler, N. (1994). The effects of voltage stability boundaries on capability charts for shunt compensated power systems. Paper presented at the Electrotechnical Conference, 1994. Proceedings., 7th Mediterranean.
19. Saha, A., Das, P., & Chakraborty, A. K. (2012). Performance analysis and comparison of various FACTS devices in power system. International Journal of Computer Applications, 46(15), 9-15.

20. Glanzmann, G., & Andersson, G. (2005). Using FACTS devices to resolve Congestions in Transmission Grids. New Orleans, LA: IEEE. 347 – 354.
21. Pandey, R., & Kori, A. (2012). Real and Reactive Power flow Control Using Flexible Ac Transmission System connected to a Transmission line: a Power Injection Concept. International Journal of Advanced Research in Computer Engineering & Technology (IJARCET), 1(6), 252-256.
22. Bhesdadiya, R., Patel, C., & Patel, R. Transmission line loadability improvement using FACTS devices. Int. J. Res. Eng. Technol.(IJRET). ISSN, 2319-1163.
23. Vishnu, J., Menon, R., Joseph, T., Sasidharan Sreedharan, V. P., Joseph, S., & Chittesh, V. (2014). Maximum loadability assessment of IEEE-14 bus system by using FACTS devices incorporating stability constraints. Paper presented at the Pro. of 2nd IRF International Conference, 10th Aug.
24. Srikumar, K., Suresh, C. V., Sivanagaraju, S., & Ganesh, V. (2014). Ordinal Optimization Approach to Power System objectives in the Presence of SVC and TCSC. International Conference on Power Systems, Energy, Environment, 185-190.
25. Nisha, P. J., & Aziz, A. (2013). Conventional/Non Linear TCSC Control Strategy for Power System Stability Enhancement. Advance in Electronic and Electric Engineering, 3(2231-1297), 389-396.